

Performance Analysis of Intelligent Reflecting Surface Assisted NOMA Networks

Xinwei Yue, *Member, IEEE* and Yuanwei Liu, *Senior IEEE*

Abstract—Intelligent reflecting surface (IRS) is a promising technology to enhance the coverage and performance of wireless networks. We consider the application of IRS to non-orthogonal multiple access (NOMA), where a base station transmits superposed signals to multiple users by the virtue of an IRS. The performance of an IRS-assisted NOMA networks with imperfect successive interference cancellation (ipSIC) and perfect successive interference cancellation (pSIC) is investigated by invoking 1-bit coding scheme. In particular, we derive new exact and asymptotic expressions for both outage probability and ergodic rate of the m -th user with ipSIC/pSIC. Based on analytical results, the diversity order of the m -th user with pSIC is in connection with the number of reflecting elements and channel ordering. The high signal-to-noise ratio (SNR) slope of ergodic rate for the m -th user is obtained. The throughput and energy efficiency of non-orthogonal users for IRS-NOMA are discussed both in delay-limited and delay-tolerant transmission modes. Additionally, we derive new exact expressions of outage probability and ergodic rate for IRS-assisted orthogonal multiple access (IRS-OMA). Numerical results are presented to substantiate our analyses and demonstrate that: i) The outage behaviors of IRS-NOMA are superior to that of IRS-OMA and relaying schemes; ii) With increasing the number of reflecting elements, IRS-NOMA is capable of achieving enhanced outage performance; and iii) The M -th user has a larger ergodic rate compared to IRS-OMA and benchmarks. However, the ergodic performance of the m -th user exceeds relaying schemes in the low SNR regime.

Index terms— Intelligent reflecting surface, non-orthogonal multiple access, imperfect SIC, 1-bit coding

I. INTRODUCTION

With the evolution of wireless communication networks, the fifth-generation (5G) and beyond has sparked a lot of concerns on high data rate, massive connectivity and spectrum utilization. The standards of 5G new radio have been completed currently and researchers are exploring the potential of emerging technologies for the next-generation communications [1–3]. As one of a promising multiple access candidate, non-orthogonal multiple access (NOMA) has the advantages in terms of spectral efficiency and link density. The distinctive feature of NOMA is that multiple users are allowed to occupy the same time/bandwidth resource blocks by utilizing the superposition coding scheme [4, 5]. It has been demonstrated that NOMA has ability to attain the better outage probability and ergodic rate compared to conventional orthogonal multiple access (OMA) [6, 7]. For the emerging

sixth-generation (6G) communication networks, it becomes pivotal to support massive intelligent equipments with different requirements.

By extending NOMA to cooperative communications, cooperative NOMA was proposed in [8], where the nearby user with better channel condition was referred to half-duplex (HD) decode-and-forward (DF) relaying to transfer the signals for the distant users. To further enhance spectrum efficiency, the authors of [9, 10] investigated the outage behavior and ergodic rate of full-duplex (FD) cooperative NOMA, where the performance of FD NOMA outperforms HD NOMA in the low signal-to-noise ratio (SNR). With the emphasis on green communication, the simultaneous wireless power transfer (SWIPT) based NOMA system was studied in [11], where the nearby user is viewed as DF relaying to forward the information. On the other hand, the authors of [12] analyzed the outage performance of a pair of users for amplify-and-forward (AF) relaying based NOMA systems. As a further development, the outage probability and ergodic performance of multiple users for AF NOMA systems were surveyed in [13, 14] over Nakagami- m fading channels. Explicit insights for understanding the impact of FD mode on AF NOMA system, the authors of [15] characterized the outage behaviors of users with an opportunistic power split factor. Apart from the above works, NOMA technique has been widely applied to multiple communication scenarios. Regarding to safety applications, the secrecy outage probability of a pair of users was analyzed in [16] for NOMA networks by invoking stochastic geometry. With the objective of improving terrestrial user connections, the authors of [17] highlighted the trajectory design and power allocation of NOMA-based unmanned aerial vehicle networks. Additionally, the application of NOMA to satellite communications was investigated [18], where the ergodic capacity and energy efficiency are derived analytically.

In view of recent attentions, intelligent reflecting surface (IRS) has been as a prospective technology for 6G wireless communications [19]. More specifically, IRS is a low-cost planar array consisting of a large of passive reflecting elements, which is ability to reconfigure the wireless propagation environment through a programmable controller. In [20], the authors proposed the concept of digital metamaterials, which manipulates the electromagnetic waves by coding ‘0’ and ‘1’ elements with control sequences (i.e., 1-bit coding). Recently, several application scenarios of IRS-aided were introduced [21] that: 1) Creating the line-of-sight (LoS) link between the BS and users via signal reflection; 2) Applying an IRS to enhance the physical layer secrecy; and 3) Deploying an IRS to realize SWIPT for a large amount of devices and so on. Similar to these paradigms, the authors of [22] surveyed

X. Yue is with the Key Laboratory of Modern Measurement & Control Technology, Ministry of Education and also with the School of Information and Communication Engineering, Beijing Information Science and Technology University, Beijing 100101, China (email: xinwei.yue@bistu.edu.cn).

Y. Liu is with the School of Electronic Engineering and Computer Science, Queen Mary University of London, London E1 4NS, U.K. (email: yuanwei.liu@qmul.ac.uk).

the symbol error probability of IRS-based communication networks in a general mathematical framework. By using intelligent reflecting elements, the authors in [23] revealed that IRS has the ability to attain high rate and energy efficiency comparing to DF relaying. As a further advance, the differences and similarities between IRS and relaying are compared in [24], which highlights the higher spectral efficiency of IRS when their size is large as relative to the wavelength of the radio waves. When the eavesdropping channels are stronger than that of legitimate channels, the authors of [25] maximized the secrecy rate of legitimate users by designing the IRS's reflecting beamforming. In [26], the energy efficient designs of IRS-based wireless communications are developed to guarantee individual link budget for users.

In light of the above discussions, researchers have begun to study the co-existence of IRS and NOMA [27–29]. Given the users' rate, the authors in [27] analyzed the IRS reflection with discrete phase shifts for IRS-aided NOMA and OMA. On the condition of user ordering, the beamforming vectors and phase shift matrix were jointly optimized to reduce the transmitting power [28]. Furthermore, the authors of [29] maximized the minimum the achievable rates of users to ensure user's fairness and improve the rate performance. For multi-antenna scenarios, the system sum rate of IRS-NOMA was improved by exploiting the fixed reflecting elements in [30]. To overcome the hardware limitations, a simple transmission of IRS-NOMA was designed in [31], where the outage probability of single user is derived with on-off control. As a further potential enhancement, the authors of [32] further studied the impact of coherent phase shifting and random phase shifting on outage behaviors for IRS-NOMA networks. In [33], the outage probability and ergodic rate of nearby user for IRS-NOMA were evaluated by designing the passive beamforming weights of IRS.

A. Motivation and Contributions

While the aforementioned significant literatures have laid a solid foundation for understanding of IRS and NOMA techniques in wireless communication networks, the treatise for enhancing the spectrum and energy efficiency by integrating these two promising technologies is a straightforward and effective approach. As stated in [20], the digital metamaterial has ability to manipulate electromagnetic waves by programming different coding sequences. Consequently, research on using the thought of 1-bit coding scheme to analyze the performance of wireless communication systems is still imperative. In addition, there are undesirable factors i.e., error propagation and quantization error in the SIC process for practical scenarios, which will result in decoding errors. It is significant to take the residual interference from SIC procedure into consideration.

Inspired by this treatise, we specifically investigate the performance of IRS-assisted NOMA with the aid of the thought of 1-bit coding, where an IRS can be regarded as a relay forwarding the information to multiple NOMA users. Moreover, we focus our attention on discussing the impact of residual interference from imperfect successive interference cancellation (ipSIC) on outage probability, ergodic rate and

energy efficiency for IRS-NOMA networks. Additionally, the outage probability and ergodic rate of IRS-OMA with 1-bit coding are surveyed carefully. According to the above explanations, the primary contributions of this paper are summarized as follows:

- 1) We derive exact and asymptotic expressions of outage probability for the m -th user with ipSIC and perfect successive interference cancellation (pSIC) in IRS-NOMA networks. Based on theoretical analyses, the diversity order for IRS-NOMA is obtained. We demonstrate that the diversity orders of the m -th user with ipSIC/pSIC are in connection with the number of reflecting elements of IRS and channel ordering. We also derive the closed-form expression of outage probability for IRS-assisted orthogonal multiple access (IRS-OMA).
- 2) We confirm that the outage behaviors of IRS-NOMA are superior to that of IRS-OMA, AF relaying and FD/HD relaying. Furthermore, we investigate the impact of IRS's deployment on the outage behaviors of IRS-NOMA networks. We observe that when the IRS is deployed closely to the BS, the enhanced outage performance is achieved. As the IRS departs from BS, the LoS deteriorates and the outage probability increases.
- 3) We derive the exact expressions of ergodic rate of the m -th user for IRS-NOMA networks. To obtain further more insights, we derive exact expression of ergodic rate for the m -th user and obtain the high SNR slopes. We observe that the ergodic rate of the m -th user converges to a throughput ceiling in the high SNR regime. As the number of reflecting elements increase, the ergodic performance of the M -th user is becoming higher compared to relaying schemes. We also derive exact expression of ergodic rate for IRS-OMA.
- 4) We study the throughput and energy efficiency of non-orthogonal users for IRS-NOMA networks in both delay-limited and delay-tolerant transmission modes. For delay-limited transmission mode, the energy efficiency of non-orthogonal users outperforms that of IRS-OMA. In delay-tolerant transmission mode, the M -th user has a larger the energy efficiency than orthogonal user and distant users. However, the energy efficiency of distant users for IRS-NOMA converges to the constant value at high SNRs.

B. Organization and Notations

The rest of this paper is organized as follows. In Section II, the network model and transmission formulation are introduced in detail. In Section III, new exact expressions of outage probability for IRS-NOMA are derived. Then the ergodic rates of IRS-NOMA are investigated in Section IV. At last, the numerical results are presented to verify theoretical analyses in Section VI and followed by concluding remarks in Section VII. The proofs of mathematics are collected in the Appendix.

The main notations used in this paper are shown as follows. $\mathbb{E}\{\cdot\}$ denotes expectation operation. $f_X(\cdot)$ and $F_X(\cdot)$ denote the probability density function (PDF) and cumulative distribution function (CDF) of a random variable X , respectively. The

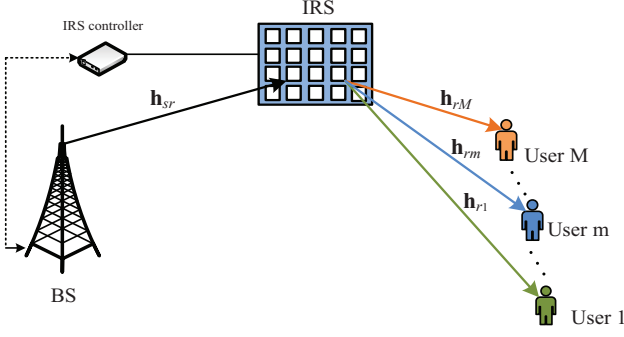


Fig. 1: An IRS-assisted downlink NOMA network model, where the communications between the BS and terminal users are completed with the help of IRS.

superscripts $(\cdot)^H$ stand for the conjugate-transpose operation. $\text{diag}(\cdot)$ represents a diagonal matrix. \otimes denotes the Kronecker product. \mathbf{I}_P is a $P \times P$ identity matrix.

II. NETWORK MODEL

A. Network Descriptions

Considering an IRS-assisted NOMA communication scenario as illustrated in Fig. 1, in which a base station (BS) sends the signals to M terminal users with the assistance of an IRS. More specifically, assuming that the direct links between BS and users are assumed strongly attenuated and the communication can be only established through the IRS. To provide the straightforward analyses, we assume that the BS and users are equipped single antenna, respectively. The IRS is mounted with K reconfigurable reflecting elements, which can be controlled by communication oriented software. The complex channel coefficient between the BS and IRS, and between the IRS and users are denoted as $\mathbf{h}_{sr} \in \mathbb{C}^{K \times 1}$ and $\mathbf{h}_{rm} \in \mathbb{C}^{K \times 1}$, respectively. All wireless links in IRS-NOMA system are modeled as Rayleigh fading channels and perturbed by additive white Gaussian noise with the mean power N_0 . Without loss of generality, the effective cascade channel gains from the BS to IRS and then to users are ordered as $|\mathbf{h}_{sr}^H \mathbf{\Theta} \mathbf{h}_{r1}|^2 \leq \dots \leq |\mathbf{h}_{sr}^H \mathbf{\Theta} \mathbf{h}_{rm}|^2 \leq \dots \leq |\mathbf{h}_{sr}^H \mathbf{\Theta} \mathbf{h}_{rM}|^2$ [7, 34], where $\mathbf{\Theta} = \text{diag}(\beta e^{j\theta_1}, \dots, \beta e^{j\theta_K}, \dots, \beta e^{j\theta_K})$ is a diagonal matrix, $\beta \in [0, 1]$ and $\theta_k \in [0, 2\pi)$ denote the fixed reflection amplitude coefficient and the phase shift of the k -th reflecting element of the IRS, respectively [21, 31]. It is noteworthy that the channel state information of all wireless channel are perfectly available at the BS. Note that imperfect channel state information is more suitable for evaluating practical scenarios, which will be set aside in our future work.

B. Signal Model

The BS sends the superposed signals to M users by the virtue of an IRS. Hence the received signal y_m reflected by IRS at the m -th user is given by

$$y_m = \mathbf{h}_{sr}^H \mathbf{\Theta} \mathbf{h}_{rm} \sum_{i=1}^M \sqrt{a_i P_s} x_i + n_m, \quad (1)$$

where x_i is assumed to be normalised the unity power signal for the i -th user, i.e., $\mathbb{E}\{x_i^2\} = 1$. The i -th user's power allocation factor a_i satisfies the relationship $a_1 \geq \dots \geq a_m \geq \dots \geq a_M$ with $\sum_{i=1}^M a_i = 1$, which is for the sake of user fairness.

The optimal power allocation coefficients between users will further heighten the performance of NOMA networks, but it is beyond the scope of this paper. P_s denotes the normalized transmission power at the BS. $\mathbf{h}_{sr} = [h_{sr}^1 \dots h_{sr}^k \dots h_{sr}^K]^H$, where $h_{sr}^k \sim \mathcal{CN}(0, \Omega_{sr})$ denotes the complex channel coefficient from the BS to the k -th reflecting element of IRS. $\mathbf{h}_{rm} = [h_{rm}^1 \dots h_{rm}^k \dots h_{rm}^K]^H$, where $h_{rm}^k \sim \mathcal{CN}(0, \Omega_{rm})$ denotes the complex channel coefficient from the k -th reflecting element of IRS to the m -th user.

On the basis of NOMA principle, the received signal-to-interference-plus-noise ratio (SINR) at the m -th user to detect the q -th user's information ($m \geq q$) is given by

$$\gamma_{m \rightarrow q} = \frac{\rho |\mathbf{h}_{sr}^H \mathbf{\Theta} \mathbf{h}_{rm}|^2 a_q}{\rho |\mathbf{h}_{sr}^H \mathbf{\Theta} \mathbf{h}_{rm}|^2 \sum_{i=q+1}^M a_i + \varpi \rho |h_I|^2 + 1}, \quad (2)$$

where $\rho = \frac{P}{N_0}$ denotes the transmit SNR and $\varpi \in [0, 1]$. More precisely, $\varpi = 0$ and $\varpi = 1$ denote the pSIC and ipSIC operations. Without loss of generality, assuming that the residual interference from ipSIC is modeled as the Rayleigh fading and corresponding complex channel coefficient is denoted by $h_I \sim \mathcal{CN}(0, \Omega_I)$.

After striking out the previous $M - 1$ users' signals with SIC, the received SINR at the M -th user to detect its own information can be given by

$$\gamma_M = \frac{\rho |\mathbf{h}_{sr}^H \mathbf{\Theta} \mathbf{h}_{rM}|^2 a_M}{\varpi \rho |h_I|^2 + 1}. \quad (3)$$

C. IRS-NOMA with 1-bit Coding

From the perspective of practical communication applications, continuously changing the reflection amplitude and phase shift of each IRS's element is beneficial to enhance the network performance. This alternative implement needs the accurate design and expensive hardware architecture, which will result in the higher cost of IRS. To facilitate implement and analysis, 1-bit coding scheme is selected to achieve the discrete amplitude/phase shift levels for IRS-assisted NOMA networks [20, 31], where the elements of diagonal matrix $\mathbf{\Theta}$ are replaced with 0 or 1. It is the scalable and cost-effective solution with the number of reflecting elements becomes larger.

Assuming that the number reflecting elements K of IRS are equal to PQ , i.e., $K = PQ$, where P and Q are integers. Define $\mathbf{V} = \mathbf{I}_P \otimes \mathbf{1}_Q$, where $\mathbf{1}_Q$ is a column vector of all ones with $Q \times 1$. The p -th column of \mathbf{V} is denoted by \mathbf{v}_p with $K \times 1$ and $\mathbf{v}_p^H \mathbf{v}_l = 0$ for $p \neq l$. As a result, the SINRs of (2) and (3) with 1-bit coding are maximized by randomly choosing \mathbf{v}_p and can be given by

$$\tilde{\gamma}_{m \rightarrow q} = \max_{\mathbf{v}_p} \frac{\rho |\mathbf{v}_p^H \mathbf{D}_m \mathbf{h}_{sr}|^2 a_q}{\rho |\mathbf{v}_p^H \mathbf{D}_m \mathbf{h}_{sr}|^2 \sum_{i=q+1}^M a_i + \varpi \rho |h_I|^2 + 1}, \quad (4)$$

and

$$\tilde{\gamma}_M = \max_{\mathbf{v}_p} \frac{\rho |\mathbf{v}_p^H \mathbf{D}_M \mathbf{h}_{sr}|^2 a_M}{\varpi \rho |h_I|^2 + 1}, \quad (5)$$

respectively, where \mathbf{D}_m and \mathbf{D}_M are the diagonal matrix with its diagonal elements obtained from \mathbf{h}_{rm} and \mathbf{h}_{rM} . The following network performance of IRS-NOMA is discussed with 1-bit coding scheme.

D. IRS-OMA

In this subsection, the IRS-OMA scheme is regarded as one of the benchmarks for comparison purpose, where an IRS is deployed to assist in the transmission from the BS to a user d . On the condition of the above assumptions, the maximized SNR of user d with 1-bit coding scheme for IRS-OMA can be given by

$$\gamma_d = \max_{\mathbf{v}_p} \rho |\mathbf{v}_p^H \mathbf{D}_d \mathbf{h}_{sr}|^2, \quad (6)$$

where $\mathbf{h}_{rd} = [h_{rd}^1 \cdots h_{rd}^k \cdots h_{rd}^K]^H$, $h_{rd}^k \sim \mathcal{CN}(0, \Omega_{rd})$ denotes the complex channel coefficient from the k -th reflecting element of IRS to user d . \mathbf{D}_d and is the diagonal matrix with its diagonal elements obtained from \mathbf{h}_{rd} .

III. OUTAGE PROBABILITY

As mentioned in conventional NOMA, the SIC scheme is carried out at the m -th user ($1 < m \leq M$) by decoding and striking out the q -th user's information ($m \geq q$) before it detects its own signal. If the m -th user cannot successfully detect the q -th user's information, an outage occurs and is denoted by

$$E_{m,q} = \left\{ \frac{\rho |\mathbf{v}_p^H \mathbf{D}_m \mathbf{h}_{sr}|^2 a_q}{\rho |\mathbf{v}_p^H \mathbf{D}_m \mathbf{h}_{sr}|^2 \sum_{i=q+1}^M a_i + \varpi \rho |h_I|^2 + 1} < \gamma_{th_q} \right\}, \quad (7)$$

where $\gamma_{th_q} = 2^{R_q} - 1$ with R_q being the target rate at the m -th user to detect x_q . As a consequence, the outage probability of m -th user with 1-bit coding for IRS-NOMA networks can be expressed as

$$P_m = \Pr[\min(E_{m,1}, E_{m,2}, \dots, E_{m,m})]. \quad (8)$$

It is worth pointing out that the first user (i.e., $m = 1$) with the worse channel condition does not execute the SIC procedure.

Theorem 1. Under Rayleigh fading channels, the closed-form expression for outage probability of the m -th user with ipSIC in IRS-NOMA networks is given by

$$P_{ipSIC}^m \approx \left\{ \phi_m \sum_{l=0}^{M-m} \sum_{u=1}^U \binom{M-m}{l} \frac{(-1)^l H_u}{m+l} \left[1 - \frac{2}{\Gamma(Q)} \right] \times \left(\frac{\psi_m^* \Lambda}{\Omega_{sr} \Omega_{rm}} \right)^{\frac{Q}{2}} K_Q \left(2 \sqrt{\frac{\psi_m^* \Lambda}{\Omega_{sr} \Omega_{rm}}} \right) \right]^{m+l} \right\}^P, \quad (9)$$

where $\phi_m = \frac{M!}{(M-m)!(m-1)!}$, $\psi_m^* = \max\{\psi_1, \dots, \psi_m\}$ and $\psi_m = \frac{\gamma_{th_m}}{\rho(a_m - \gamma_{th_m} \sum_{i=m+1}^M a_i)}$ with $a_m > \gamma_{th_m} \sum_{i=m+1}^M a_i$. $\gamma_{th_m} = 2^{R_m} - 1$ with R_m being the target rate at the m -th user to detect x_m . $\Lambda = (\varpi \rho \Omega_I x_u + 1)$. H_u and r_u are the weight and abscissas for the Gauss-Laguerre integration, respectively. More specifically, r_u is the w -th zero of Laguerre polynomial $L_U(r_u)$ and the corresponding the w -th weight is given by $H_u = \frac{(U!)^2 r_u}{[L_{U+1}(r_u)]^2}$. The parameter U is to ensure a complexity-accuracy tradeoff. $K_v(\cdot)$ is the modified Bessel function of the second kind with order v . $\Gamma(\cdot)$ denotes the gamma function [35, Eq. (8.310.1)].

Proof. See Appendix A. \square

Corollary 1. For the special case with substituting $\varpi = 0$ into (A.2), the closed-form expression for outage probability of the m -th user with pSIC in IRS-NOMA networks is given by

$$P_{pSIC}^m = \left\{ \phi_m \sum_{l=0}^{M-m} \binom{M-m}{l} \frac{(-1)^l}{m+l} \left[1 - \frac{2}{\Gamma(Q)} \right] \times \left(\frac{\psi_m^*}{\Omega_{sr} \Omega_{rm}} \right)^{\frac{Q}{2}} K_Q \left(2 \sqrt{\frac{\psi_m^*}{\Omega_{sr} \Omega_{rm}}} \right) \right]^{m+l} \right\}^P. \quad (10)$$

For IRS-OMA, an outage is defined as the probability that the instantaneous SNR (γ_d) falls bellow a threshold SNR γ_{th_d} . Hence the outage probability of user d with 1-bit coding which can be expressed as

$$P_d = \Pr(\gamma_d \leq \gamma_{th_d}), \quad (11)$$

where $\gamma_{th_d} = 2^{R_{oma}} - 1$ with R_{oma} being the target rate of user d to detect x_d . Referring to (10) and removing the order operation, we can derive the outage probability for IRS-OMA in the following corollary.

Corollary 2. The closed-form expression of outage probability for IRS-OMA networks with 1-bit coding is given by

$$P_d = \left[1 - \frac{2}{\Gamma(Q)} \left(\frac{\gamma_{th_d}}{\rho \Omega_{sr} \Omega_{rd}} \right)^{\frac{Q}{2}} K_Q \left(2 \sqrt{\frac{\gamma_{th_d}}{\rho \Omega_{sr} \Omega_{rd}}} \right) \right]^P. \quad (12)$$

A. Diversity Analysis

In order to gain better insights, the diversity order is usually selected to evaluate the outage behaviors for communication systems, which is able to describe how fast the outage probability decreases with the transmitting SNR. Hence the diversity order can be expressed as

$$d = - \lim_{\rho \rightarrow \infty} \frac{\log(P_\infty(\rho))}{\log \rho}, \quad (13)$$

where $P_\infty(\rho)$ denotes the asymptotic outage probability in the high SNR regime.

Corollary 3. Based on analytical result in (9), when $\rho \rightarrow \infty$, the asymptotic outage probability of the m -th user with ipSIC for IRS-NOMA networks is given by

$$P_{ipSIC}^{m,\infty} \approx \left\{ \frac{M!}{(M-m)!m!} \sum_{w=1}^W H_w \left[1 - \frac{2}{\Gamma(Q)} \right] \times \left(\frac{\varpi \vartheta_m^* \Omega_I x_w}{\Omega_{sr} \Omega_{rm}} \right)^{\frac{Q}{2}} K_Q \left(2 \sqrt{\frac{\varpi \vartheta_m^* \Omega_I x_w}{\Omega_{sr} \Omega_{rm}}} \right) \right\}^m \Bigg\}^P, \quad (14)$$

where $\vartheta_m^* = \max\{\vartheta_1, \dots, \vartheta_m\}$ and $\vartheta_m = \frac{\gamma_{thm}}{(a_m - \gamma_{thm} \sum_{i=m+1}^M a_i)}$ with $a_m > \gamma_{thm} \sum_{i=m+1}^M a_i$.

Remark 1. Upon substituting (14) into (13), the diversity order of the m -th user with ipSIC for IRS-NOMA is equal to zero. This is due to the influence of residual interference from ipSIC.

Corollary 4. For the cases $Q = 1$ and $Q \geq 2$, the asymptotic outage probability of the m -th user with pSIC at high SNRs are given by

$$P_{pSIC}^{m,\infty} = \left\{ \frac{M!}{(M-m)!m!} \left[-\frac{2\psi_m^*}{\Omega_{sr} \Omega_{rm}} \times \ln \left(\sqrt{\frac{\psi_m^*}{\Omega_{sr} \Omega_{rm}}} \right) \right]^m \right\}^K, \quad Q = 1, \quad (15)$$

and

$$P_{pSIC}^{m,\infty} = \left\{ \frac{M!}{(M-m)!m!} \times \left(\frac{\psi_m^*}{(Q-1)\Omega_{sr} \Omega_{rm}} \right)^m \right\}^P, \quad Q \geq 2, \quad (16)$$

respectively.

Proof. To facilitate the calculation, we employ the series representation of Bessel functions $K_v(x)$ to obtain the high SNR approximation. When $v = 1$ and $v \geq 2$, $K_v(x)$ can be approximated as

$$K_1(x) \approx \frac{1}{x} + \frac{x}{2} \ln \left(\frac{x}{2} \right), \quad (17)$$

and

$$K_v(x) \approx \frac{1}{2} \left[\frac{2^v (v-1)!}{x^v} - \frac{2^{v-2} (v-2)!}{x^{v-2}} \right], \quad (18)$$

respectively. Upon substituting (17) and (18) into (10), and then taking the first term ($l = 0$) of summation term, we can obtain (15) and (16), respectively. The proof is completed. \square

Remark 2. Upon substituting (15) and (16) into (13), the diversity orders of the m -th user with pSIC for cases $Q = 1$ and $Q \geq 2$ are mK and mP , respectively. As can be observed that the diversity order of the m -th user are in connection with the number of reflecting elements of IRS and channel ordering.

Corollary 5. Similar to the procedures in (15) and (16), the asymptotic outage probability of IRS-OMA for both $Q = 1$ and $Q \geq 2$ at high SNRs are given by

$$P_d^\infty = \left[-2 \left(\frac{\gamma_{thd}}{\rho \Omega_{sr} \Omega_{rd}} \right) \ln \left(\sqrt{\frac{\gamma_{thd}}{\rho \Omega_{sr} \Omega_{rd}}} \right) \right]^K, \quad Q = 1, \quad (19)$$

and

$$P_d^\infty = \left[\frac{\gamma_{thd}}{\rho (Q-1) \Omega_{sr} \Omega_{rd}} \right]^P, \quad Q \geq 2, \quad (20)$$

respectively.

Remark 3. Upon substituting (19) and (20) into (13), the diversity orders of IRS-OMA with 1-bit coding for cases $Q = 1$ and $Q \geq 2$ are K and P , respectively.

B. Delay-Limited Transmission

In the delay-limited transmission mode, the BS sends the information at a constant rate, which is subject to outage according to the random fading of wireless channels [9, 36]. Hence the throughput of the m -th user with ipSIC/pSIC for IRS-NOMA networks in the delay-limited transmission mode can be given by

$$R_{m,dl} = (1 - P_\xi^m) R_m, \quad (21)$$

where $\xi \in \{ipSIC, pSIC\}$. P_m^{ipSIC} and P_m^{pSIC} can be obtained from (9) and (10), respectively.

IV. ERGODIC RATE

In this section, the ergodic rate of the m -th user with ipSIC/pSIC for IRS-NOMA networks is discussed in detail, where the target rates of users are determined by the channel conditions. The m -th user detects the p -th user's information successfully, since it holds $|\mathbf{h}_{sr}^H \Theta \mathbf{h}_{rm}|^2 \geq |\mathbf{h}_{sr}^H \Theta \mathbf{h}_{rp}|^2$. Under this situation, the achievable rate of the m -th user can be written as $\tilde{R}_m = \log(1 + \tilde{\gamma}_{m \rightarrow m})$. Based on (4) and (5), the ergodic rates of the m -th user and the M -th user with ipSIC for IRS-NOMA networks can be given by

$$R_{m,erg}^{ipSIC} = \mathbb{E} \left\{ \log \left(1 + \max_{\mathbf{v}_p} \frac{\rho |\mathbf{v}_p^H \mathbf{D}_m \mathbf{h}_{sr}|^2 a_m}{\rho |\mathbf{v}_p^H \mathbf{D}_m \mathbf{h}_{sr}|^2 \bar{a}_m + \varpi \rho |h_I|^2 + 1} \right) \right\}, \quad (22)$$

and

$$R_{M,erg}^{ipSIC} = \mathbb{E} \left\{ \log \left(1 + \max_{\mathbf{v}_p} \frac{\rho |\mathbf{v}_p^H \mathbf{D}_M \mathbf{h}_{sr}|^2 a_M}{\varpi \rho |h_I|^2 + 1} \right) \right\}, \quad (23)$$

respectively, where $\varpi = 1$ and $\bar{a}_m = \sum_{i=m+1}^M a_i$. One can be seen from the equations, there are no the closed-form solutions. However, these expressions can be evaluated numerically by using the standard softwares such as Matlab or Mathematica. By employing pSIC, the ergodic rates of the m -th user and the M -th user are presented in the following part.

Theorem 2. For the special case with substituting $\varpi = 0$ into (22), the closed-form expression of ergodic rate for the m -th user with pSIC in IRS-NOMA networks is given by

$$R_{m,erg}^{pSIC} \approx \frac{\pi a_m}{N \ln 2} \sum_{n=1}^N \frac{\sqrt{1-x_n^2}}{2\bar{a}_m + (1+x_n)a_m} \langle 1 - \{\phi_m \times \sum_{l=0}^{M-m} \sum_{r=0}^{m+l} \binom{M-m}{l} \binom{m+l}{r} \frac{(-1)^{l+r}}{m+l} \left(\frac{2}{\Gamma(Q)}\right)^r \times \left[\left(\frac{\varphi_m(1+x_n)}{\bar{a}_m(1-x_n)} \right)^{\frac{Q}{2}} K_Q \left(2\sqrt{\frac{\varphi_m(1+x_n)}{\bar{a}_m(1-x_n)}} \right) \right]^r \}^P \rangle, \quad (24)$$

where $\phi_m = \frac{M!}{(M-m)!(m-1)!}$, $\varphi_m = \frac{1}{\rho\Omega_{sr}\Omega_{rm}}$, $x_n = \cos\left(\frac{2n-1}{2N}\pi\right)$ and N is a parameter to ensure a complexity-accuracy tradeoff.

Proof. See Appendix B. \square

Theorem 3. For the special case with substituting $\varpi = 0$ into (23), the exact expression of ergodic rate for the M -th user with pSIC in IRS-NOMA networks is given by

$$R_{M,erg}^{pSIC} = \frac{\rho a_M}{\ln 2} \sum_{r=1}^{MP} \binom{MP}{r} \frac{(-1)^{r+1} 2^r}{\left[\Gamma(Q) (\Omega_{sr}\Omega_{rM})^{\frac{Q}{2}} \right]^r} \times \int_0^\infty \frac{x^{\frac{rQ}{2}} \left[K_Q \left(2\sqrt{\frac{x}{\Omega_{sr}\Omega_{rM}}} \right) \right]^r}{1 + \rho a_M x} dx. \quad (25)$$

Proof. See Appendix C. \square

For IRS-OMA, based on (6), the ergodic rate of user d with 1-bit coding can be expressed as

$$R_{d,erg} = \mathbb{E} \left[\log \left(1 + \max_{\mathbf{v}_p} \rho |\mathbf{v}_p^H \mathbf{D}_d \mathbf{h}_{sd}|^2 \right) \right]. \quad (26)$$

Corollary 6. Similar to the derivation process in (25), the exact expression of ergodic rate for IRS-OMA with 1-bit coding is given by

$$R_{d,erg} = \frac{\rho}{\ln 2} \sum_{r=1}^P \binom{P}{r} \frac{(-1)^{r+1} 2^r}{\left[\Gamma(Q) (\Omega_{sr}\Omega_{rd})^{\frac{Q}{2}} \right]^r} \times \int_0^\infty \frac{x^{\frac{rQ}{2}} \left[K_Q \left(2\sqrt{\frac{x}{\Omega_{sr}\Omega_{rd}}} \right) \right]^r}{1 + \rho x} dx. \quad (27)$$

A. Slope Analysis

Similar to the diversity order, the high SNR slope aims to capture the diversification of ergodic rate with the transmitting SNRs, which can be defined as

$$S = \lim_{\rho \rightarrow \infty} \frac{R_m^\infty(\rho)}{\log(\rho)}, \quad (28)$$

where $R_m^\infty(\rho)$ denotes the asymptotic ergodic rate in the high SNR regime.

According to (B.1), when $\rho \rightarrow \infty$, the asymptotic ergodic rate of the m -th user with pSIC is given by

$$R_{erg}^{m,\infty} = \log \left[1 + \left(\frac{a_m}{\bar{a}_m} \right) \right]. \quad (29)$$

Remark 4. Upon substituting (29) into (28), the high SNR slope of the m -th user with pSIC for IRS-NOMA networks is zero, which is the same as conventional NOMA.

As can be seen from (25) that the exact derivation of the approximation at high SNRs appears mathematically intractable. Furthermore, we focus our attention on evaluating the slope of ergodic rate for the M -th user via the assistance of its upper bound. By noticing that $\log(1+x^2)$ is a concave function for $x \geq 0$, we invoke the Jensens inequality to derive an upper bound as

$$R_{M,erg}^{pSIC} \leq \log \left[1 + \rho a_M \mathbb{E} \left(\max_{\mathbf{v}_p} |\mathbf{v}_p^H \mathbf{D}_M \mathbf{h}_{sr}|^2 \right) \right]. \quad (30)$$

We perform the derivative operation on (C.3) in Appendix C and some manipulates, the upper bound $R_{M,erg}^{pSIC,ub}$ is given by

$$R_{M,erg}^{pSIC,ub} = \log \left\{ 1 + \frac{2MP\Phi a_M \rho}{\Gamma(Q) (\sqrt{\Omega_{sr}\Omega_{rM}})^{Q+1}} \right\}, \quad (31)$$

where $\Phi = \int_0^\infty \left[1 - \frac{2}{\Gamma(Q)} \left(\frac{x}{\Omega_{sr}\Omega_{rM}} \right)^{\frac{Q}{2}} K_Q \left(\sqrt{\frac{4x}{\Omega_{sr}\Omega_{rM}}} \right) \right]^{MP-1} \times x^{\frac{Q-1}{2}} K_{Q-1} \left(2\sqrt{\frac{x}{\Omega_{sr}\Omega_{rM}}} \right) dx$ is constant with increasing the SNRs. Upon substituting (31) into (28) and further applying L'hospital rule, we can obtain the high SNR slope of ergodic rate for the M -th user in the following remark.

Remark 5. Upon substituting (31) into (28), the high SNR slope of the M -th user with pSIC for IRS-NOMA networks is equal to one. One can observe that the use of IRS to NOMA donot improve the slope of ergodic rate for the M -th user.

B. Delay-Tolerate Transmission

In the delay-tolerant mode, the BS sends the information at any fixed rate upper bounded by the ergodic capacity. Hence the throughput of the m -th user and the M -th user with pSIC for IRS-NOMA networks is given by

$$R_{\zeta,dt} = R_{\zeta,erg}^{pSIC}, \quad (32)$$

where $\zeta \in \{m, M\}$. $R_{m,erg}^{pSIC}$ and $R_{M,erg}^{pSIC}$ can be obtained from (24) and (25), respectively.

To facilitate comparison, the diversity orders and high SNR slopes of the m -th user with ipSIC/pSIC for IRS-NOMA are summarized in TABLE I, where we use “D” and “S” to represent the diversity order and high SNR slope, respectively.

Mode	SIC	User	D	S
IRS-OMA	—	User d ($Q=1$)	K	—
		User d ($Q \geq 2$)	P	—
IRS-NOMA	ipSIC	User m	0	—
	pSIC	User m ($Q=1$)	mK	0
		User m ($Q \geq 2$)	mP	0

TABLE I: Diversity order and high SNR slope for IRS-NOMA networks.

TABLE II: Table of Parameters for Numerical Results

Monte Carlo simulations repeated	10^6 iterations
Pass loss exponent	$\alpha = 2$
The power allocation factors for users	$a_1 = 0.5$
	$a_2 = 0.4$
	$a_3 = 0.1$
The targeted data rates for users	$R_1 = 0.6$ BPCU
	$R_2 = 1.6$ BPCU
	$R_3 = 2$ BPCU
The distance from BS to IRS	$d_{sr} = 0.5$
The distance from IRS to users	$d_{r1} = 0.5$
	$d_{r2} = 0.4$
	$d_{r3} = 0.3$

V. ENERGY EFFICIENCY

In wireless communication systems, the energy efficiency (EE) can be interpreted as the user's data rate divided by the energy consumption, which can be expressed as

$$\eta_{EE} = \frac{\text{Data rate}}{\text{Energy consumption}}. \quad (33)$$

More specifically, based on above throughput analyses, the energy efficiency of IRS-NOMA networks is given by

$$\eta = \frac{R_\Phi}{TP_s}, \quad (34)$$

where $R_\Phi \in (R_{m,dl}, R_{\zeta,dt})$ and T denotes the entire communication process time.

VI. NUMERICAL RESULTS

In this section, the numerical results are presented to confirm the rationality of the derived theoretical expressions for IRS-NOMA networks. We show the impact of the reflecting elements on the performance of the IRS-NOMA communication network. Monte Carlo simulation parameters used are summarized in TABLE II, where BPCU denotes the short for bit per channel use. Assume that three users $M = 3$ are taken into consideration and the distance from the BS to IRS, and then to the terminal users are normalized to unity. As a further development, the variances of complex channel coefficients are set to be $\Omega_{sr} = d_{sr}^{-\alpha}$, $\Omega_{r1} = d_{r1}^{-\alpha}$, $\Omega_{r2} = d_{r2}^{-\alpha}$ and $\Omega_{r3} = d_{r3}^{-\alpha}$, respectively. The complexity-vs-accuracy tradeoff parameter is set to be $N = 20$ and simulation results are denoted by \bullet . Without loss of the generality, the IRS-OMA and conventional OMA (i.e., variable gain AF relaying, FD/HD DF relaying) are selected as the benchmarks for the purpose of comparison. Here AF relaying works in HD mode and is equipped with a single antenna. The FD DF relaying is equipped with one transmit antenna and one receive antenna, while HD DF relaying has a single antenna. The target rate R_{oma} of the orthogonal user is equal to $\sum_{i=1}^M R_i$.

A. Outage Probability

Fig. 2 plots the outage probability of three users versus SNR for a simulation setting with $K = 1$, $Q = 1$, $P = 1$, $R_1 = 0.6$, $R_2 = 1.6$, $R_3 = 2$ and $R_{oma} = 4.2$ BPCU. The theoretical analysis curves of outage probability for users with pSIC are plotted according to (10). It is obvious that the Monte

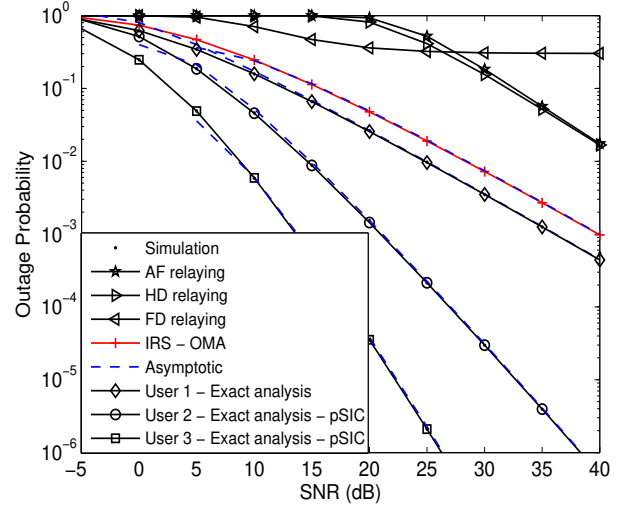


Fig. 2: Outage probability versus the transmit SNR, with $K = 1$, $Q = 1$, $P = 1$, $R_1 = 0.6$, $R_2 = 1.6$, $R_3 = 2$ and $R_{oma} = 4.2$ BPCU.

Carlo simulation outage probability curves excellently agree with analytical results across the entire average SNR range. The asymptotic outage probability converges to the analytical expressions given in (16), which proves the effectiveness of our theoretical derivation. As can be seen from the figure that the outage performance of the nearest user ($m = 3$) is higher than that of the distant users ($m = 2$ and $m = 1$). This is due to the fact that the nearby user attains the higher diversity order, which verifies the insights in **Remark 2**. The exact and asymptotic outage probability curves of IRS-OMA are plotted according to the analytical results in (12) and (19), respectively. One can observe that the outage behaviors of IRS-NOMA with pSIC are superior than that of IRS-OMA (12), variable gain AF relaying [37], FD relaying [38, Eq. (7)] with loop self-interference i.e., $\mathbb{E}\{|h_{LI}|^2\} = -10$ dB and HD relaying [38, Eq. (8)]. The reasons are that: 1) IRS-NOMA can realize much better user fairness than IRS-OMA for multiple users; 2) FD DF relay suffers from loop interference due to signal leakage and needs the advanced loop interference cancellation technologies, which will lead to the higher cost; and 3) IRS-NOMA operates in FD mode provides the more spectrum efficient than HD DF relaying.

Fig. 3 plots the outage probability of three users versus SNR for a simulation setting with $K = 2$, $Q = 2$, $P = 1$, $\varpi = 1$, $R_1 = 0.6$, $R_2 = 1.6$, $R_3 = 2$ and $R_{oma} = 4.2$ BPCU. The exact and approximate analyses curves of outage probability for users with ipSIC are plotted by (9) and (14), respectively. The exact and asymptotic outage probability curves of IRS-OMA are plotted by (12) and (20), respectively. The simulation results matches closely with the theoretical analysis. The important observation is that the outage probability of distant users with ipSIC converges to an error floor in the high SNR regime and thus obtain a zero diversity order. The reason is that there is the residual interference from ipSIC for IRS-NOMA. This phenomenon is also confirmed by the conclusions in

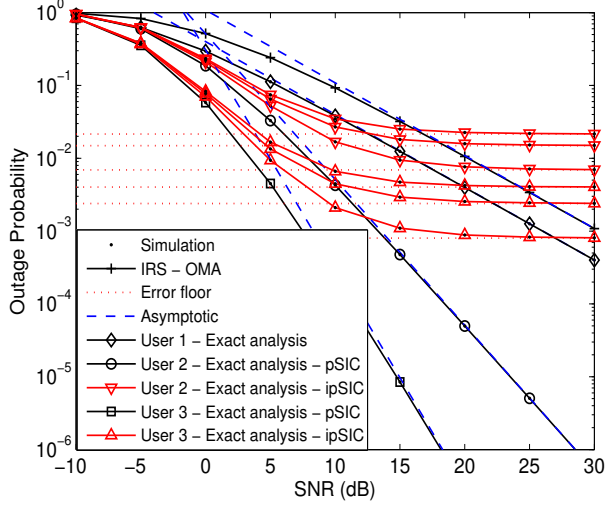


Fig. 3: Outage probability versus the transmit SNR with different residual interference, $K = 2$, $Q = 2$, $P = 1$, $R_1 = 0.6$, $R_2 = 1.6$, $R_3 = 2$ and $R_{oma} = 4.2$ BPCU.

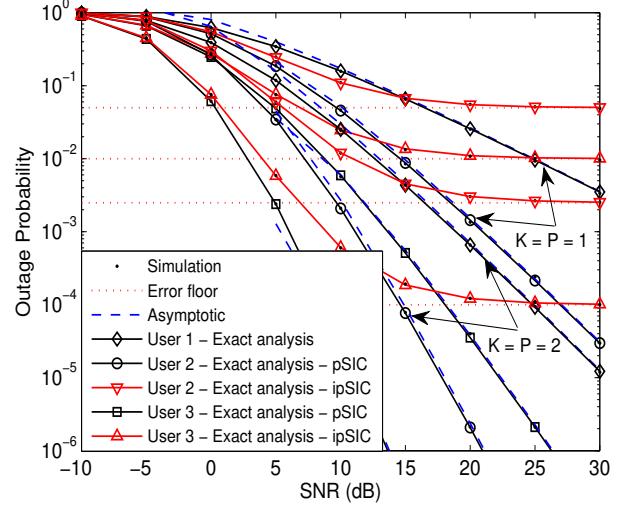


Fig. 5: Outage probability versus the transmit SNR, with $\varpi = 1$, $Q = 1$, $R_1 = 0.6$, $R_2 = 1.6$, $R_3 = 2$ BPCU and $\mathbb{E}\{|h_I|^2\} = -10$ dB.

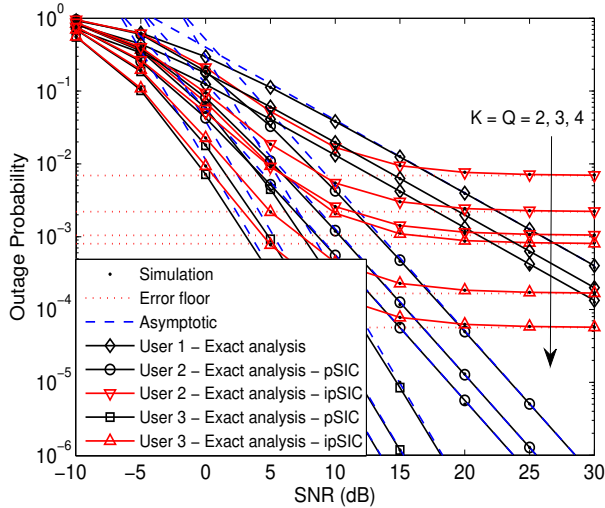


Fig. 4: Outage probability versus the transmit SNR, with $P = 1$, $\varpi = 1$, $R_1 = 0.6$, $R_2 = 1.6$, $R_3 = 2$ BPCU and $\mathbb{E}\{|h_I|^2\} = -10$ dB.

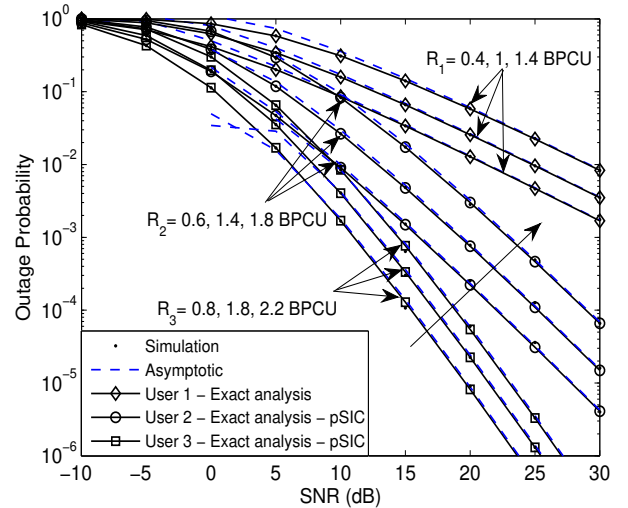


Fig. 6: Outage probability versus the transmit SNR, with the different target rate for $K = 2$, $P = 2$ and $Q = 1$.

Remark 1. Additionally, it is worth noting that the farthest user ($m = 1$) does not carry out the SIC operation, since it has the worst channel conditions. Compared to the benchmark of IRS-OMA, we observe that IRS-NOMA with ipSIC is also capable of achieving the lower outage behaviors. Certainly, with the value of residual interference increasing, the achieved outage probability of IRS-NOMA converges to the worst error floors. As a result, it is important to consider the influence of ipSIC on the network performance for IRS-NOMA in the practical scenario.

Fig. 4 plots the outage probability versus SNR for a simulation system with different reflecting elements of IRS and $\mathbb{E}\{|h_I|^2\} = -10$ dB. One can observe that the setting of the

reflecting elements for IRS-NOMA is significant to provide the network performance. With increasing the number of reflecting elements K , the lower outage probabilities are attained for multiple users. This behaviors are caused by the fact that the application of IRS to NOMA networks provides a new degree of freedom to enhance the wireless link performance. This phenomenon is also certificate the completion of **Remark 2**, where both the number of reflecting elements and channel ordering determine the slope of outage probability for IRS-NOMA. Another observation is that all outage probability curves of each user have the same slopes, which manifests that the diversity orders of users are the same. This appearance demonstrates the insight we derived from the analytical results given by (16).

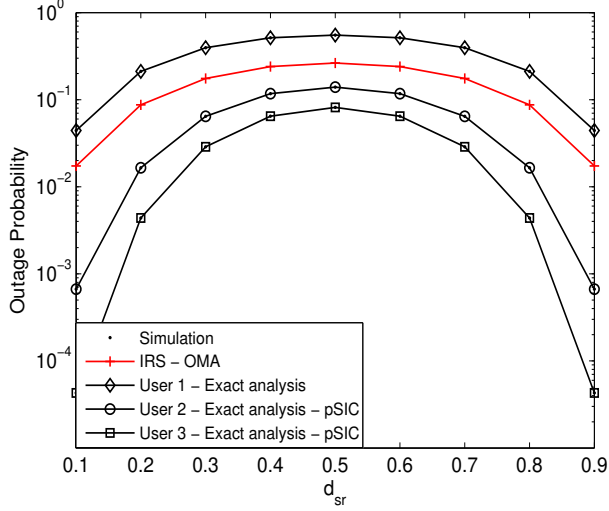


Fig. 7: Outage probability versus distance d_{sr} between the BS and IRS, with $Q = 2$, $K = 2$, $P = 1$, $R_1 = R_2 = R_3 = 0.6$ BPCU, $R_{oma} = 1.8$ BPCU.

Fig. 5 plots the outage probability versus SNR for a simulation setting with $Q = 1$, $\varpi = 1$, $R_1 = 0.6$, $R_2 = 1.6$, $R_3 = 2$ BPCU and $\mathbb{E}\{|h_I|^2\} = -10$ dB. The approximated outage probability curves of users are plotted corresponding to (15), which match precisely with the simulation results. As can be observed from the figure that as the number of reflecting elements increases, the outage probability of users is becoming much smaller. The main reason behind this is that IRS-NOMA with 1-bit coding provides much more diversity orders given by **Remark 2**. It is worth mentioning that the outage probability curves of each user has a different diversity order, which confirms the analytical result derived in (15). Fig. 6 plots the outage probability versus SNR with the different target rate for $K = 2$, $P = 2$ and $Q = 1$. One can observe that adjusting the target rate of users largely affect the outage performance. With the values of target rate increasing, the outage behaviors of users for IRS-NOMA networks are becoming much worse, which is in line with the conventional NOMA networks [7].

To illustrate the impact of IRS's deployment on the performance, Fig. 7 plots the outage probability as a function of the normalized distance between the BS and users, with $Q = 2$, $K = 2$, $P = 1$, $R_1 = R_2 = R_3 = 0.6$ BPCU, $R_{oma} = 1.8$ BPCU. We can observe that when the IRS is deployed closely to BS, the outage performance of non-orthogonal users is becoming much better. This phenomenon can be explained that the IRS can receive the clear LoS signals from the BS for the purpose of maximizing its received signal power. As the IRS departs from BS, the LoS deteriorates and outage probability of users increases seriously. When the IRS is in the middle of the BS and users, the worst outage behaviors of users are attained in the IRS-NOMA networks. This is due to the fact that the IRS is neither closed to the BS nor to users. After this point, the performance begins to improve again. This is because that the IRS is close to NOMA users and enhance the

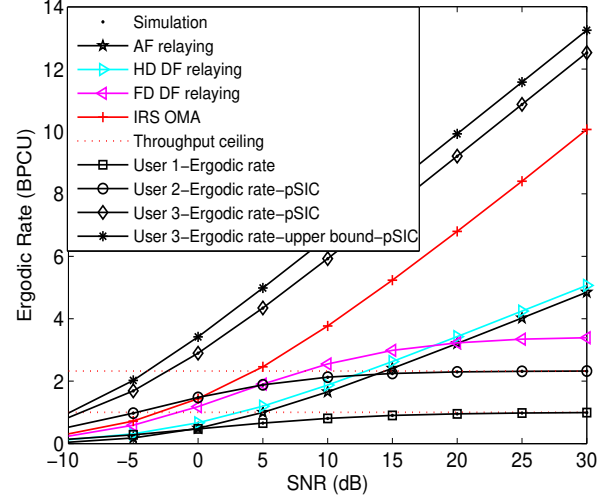


Fig. 8: Rates versus the transmit SNR, with $K = 1$, $Q = 1$ and $P = 1$.

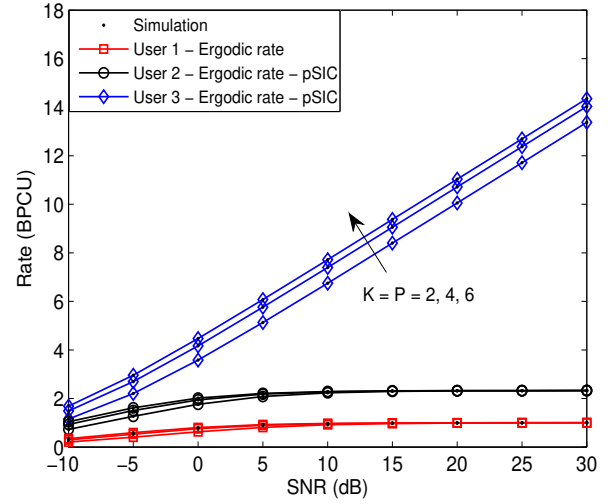


Fig. 9: Rates versus the transmit SNR, with $Q = 1$.

reflecting signals received by users. Such an outage behavior can be useful to establish an optimal deployment of IRS in NOMA networks. As a consequence, the deployment scenarios of IRS should take into account some practical constraints.

B. Ergodic Rate

Fig. 8 plots the ergodic rates versus SNR, with $K = 1$, $Q = 1$ and $P = 1$. The exact curves of ergodic rate for the m -th user and M -th user with pSIC are plotted based on (24) and (25), respectively. One can observe that the ergodic rates of distant users for IRS-NOMA outperform that of AF relaying and FD/HD relaying in the low SNR regime, which are consistent to FD/HD NOMA systems [9, 10]. As the SNR value increases, the ergodic rate of distant users converges to a throughput ceiling, which is also confirmed in **Remark 4**. This is due to the fact that the distant user will suffer

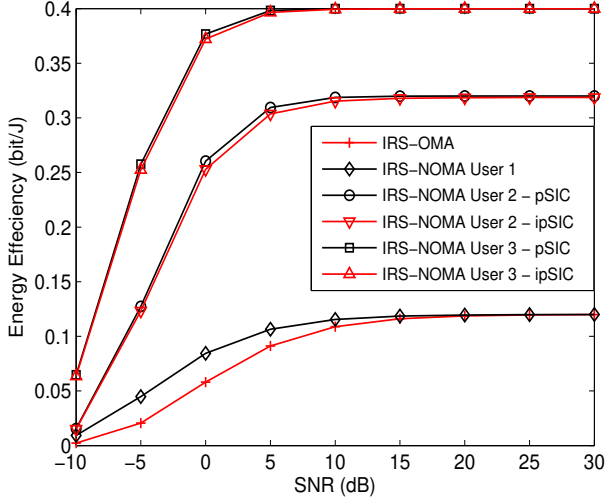


Fig. 10: Energy efficiency in delay-limited transmission mode, where $P_s = 5$ W and $T = 1$.

from the interference from the nearby users' signals when it decodes their own signals. Another observation is that the ergodic rate of nearest user is much greater than that of non-orthogonal users, IRS-OMA (27), AF relaying and FD/HD relaying. The origin for this behavior is that it is closest to the IRS and has the best channel conditions. In addition, Fig. 9 plots the ergodic rates versus SNR with different reflecting elements. As can be observed from this figure that with the increasing reflecting elements of IRS, the ergodic performance of the nearest user with pSIC is enhanced and has the same slopes, which confirms the insights in **Remark 5**. The distant users' performance has no obvious variety due to the effects of interference signals. We conclude that IRS-NOMA cannot circumvent the problem of *zero* slope for the distant users.

C. Energy Efficiency

Fig. 10 plots the energy efficiency for IRS-NOMA networks in the delay-limited transmission mode, with $P_s = 5$ W and $T = 1$. The energy efficiency curve of non-orthogonal users for IRS-NOMA with ipSIC/pSIC is plotted according to (34). It can be observed that the energy efficiency of non-orthogonal users outperforms that of IRS-OMA. This is because that non-orthogonal users is capable of achieving the larger data rate in the delay-limited transmission mode. This phenomenon indicates that IRS-NOMA networks have the ability to supply the higher energy efficiency. As a further advance, Fig. 11 plots the energy efficiency for IRS-NOMA in delay-tolerant transmission mode, with $P_s = 15$ W and $T = 1$. We observe that the energy efficiency of nearest user is much larger than that of orthogonal user and distant users. This is due to that the nearest user is closed to the IRS and has a greater throughput. Another observation is that the energy efficiency of distant users for IRS-NOMA converges to the constant value at high SNRs. The reason is that the distant users suffer from the nearby user's interference, when it detects its own information.

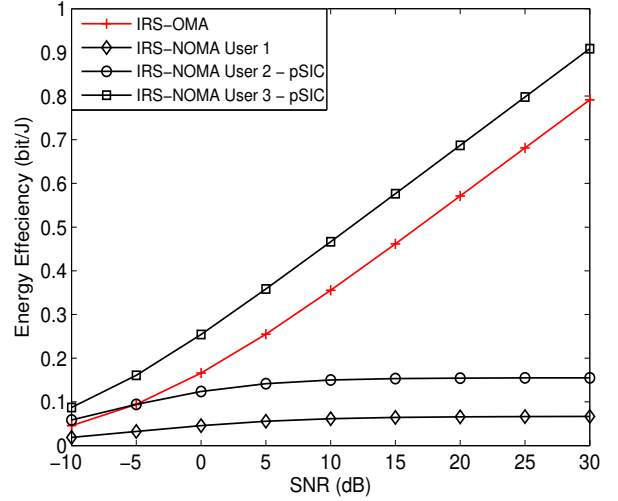


Fig. 11: Energy efficiency in delay-tolerant transmission mode, where $P_s = 15$ W and $T = 1$.

VII. CONCLUSION

In this paper, an IRS has been invoked in downlink NOMA networks for enhancing the performance of multiple users, where 1-bit coding scheme is taken into account. More specifically, we have derived the exact expressions of outage probability and ergodic rate for users with ipSIC/pSIC in IRS-assisted NOMA networks. Based on the approximated analyses, the diversity order of the m -th user is related to the number of reflecting elements and channel ordering. With increasing the number of reflecting elements, the outage probability of users with ipSIC/pSIC for IRS-NOMA networks decreases. Due to the interference from the nearby users' signals, a *zero* of high SNR slope for ergodic rate is obtained by the distant users. Simulation results have shown that the outage behaviors of IRS-NOMA are superior to that of IRS-OMA, AF relaying and FD/HD DF relaying. The nearest user has a larger ergodic rate than orthogonal user and distant users. Finally, the throughput and energy efficiency of non-orthogonal users for IRS-NOMA were discussed both in delay-limited and delay-tolerant transmission modes. The application of IRS to NOMA provided a new degree of freedom to enhance the wireless link performance.

APPENDIX A: PROOF OF THEOREM 1

The proof starts by assuming $W_p = \min(E_{m,1}, E_{m,2}, \dots, E_{m,m})$, $W = \max(W_1, W_2, \dots, W_P)$ and then

$$\begin{aligned} P_m &= \Pr(W) = \Pr[\max(W_1, W_2, \dots, W_P)] \\ &= \prod_{p=1}^P \Pr(W_p) = [\Pr(W_p)]^P. \end{aligned} \quad (\text{A.1})$$

Hence the outage probability of the m -th user with ipSIC need to further calculate $\Pr(W_p)$. Applying the complementary set

and some algebraic manipulations, it can be calculated as follows:

$$\begin{aligned} \Pr(W_p) &= \Pr\left[|\mathbf{v}_p^H \mathbf{D}_m \mathbf{h}_{sr}|^2 < \psi_m^* (\varpi \rho |h_I|^2 + 1)\right] \\ &= \int_0^\infty F_{|\mathbf{v}_p^H \mathbf{D}_m \mathbf{h}_{sr}|^2}(\psi_m^* (\varpi \rho y + 1)) f_{|h_I|^2}(y) dy, \quad (\text{A.2}) \end{aligned}$$

where $\varpi = 1$, $f_{|h_I|^2}(y) = \frac{1}{\Omega_I} e^{-\frac{y}{\Omega_I}}$, $\psi_m^* = \max\{\psi_1, \dots, \psi_m\}$ with $a_m > \gamma_{th_m} \sum_{i=m+1}^M a_i$ and $\psi_m = \frac{\gamma_{th_m} \sum_{i=m+1}^M a_i}{\rho(a_m - \gamma_{th_m} \sum_{i=m+1}^M a_i)}$. Based on the previous assumption, the cascade channel gains from the BS to IRS and then to users with 1-bit coding scheme are also sorted as $|\mathbf{v}_p^H \mathbf{D}_1 \mathbf{h}_{sr}|^2 \leq \dots \leq |\mathbf{v}_p^H \mathbf{D}_m \mathbf{h}_{sr}|^2 \leq \dots \leq |\mathbf{v}_p^H \mathbf{D}_M \mathbf{h}_{sr}|^2$. As a further advance, we focus our attention the CDF $F_{|\mathbf{v}_p^H \mathbf{D}_m \mathbf{h}_{sr}|^2}(x)$ in the following part.

Denoting $X = |\mathbf{v}_p^H \mathbf{D}_m \mathbf{h}_{sr}|^2$, the CDF $F_X(x)$ of the cascade channel gain has a fixed relationship with the unsorted channel gain [7, 34], which can be expressed as

$$\begin{aligned} F_X(x) &= \frac{M!}{(M-m)!(m-1)!} \sum_{l=0}^{M-m} \binom{M-m}{l} \\ &\quad \times \frac{(-1)^l}{m+l} [\bar{F}_X(x)]^{m+l}, \quad (\text{A.3}) \end{aligned}$$

where $\bar{F}_X(x)$ denotes the CDF of unsorted cascade channel gain. After some arithmetical manipulations, we can further express $X = \left|\sum_{k=1}^Q h_{sr}^k h_{rm}^k\right|^2$, where $h_{sr}^k \sim \mathcal{CN}(0, \Omega_{sr})$ and $h_{rm}^k \sim \mathcal{CN}(0, \Omega_{rm})$. Based on [39, Eq. (7)], the PDF $\bar{f}_X(x)$ of the cascade channel gain $X = |\mathbf{v}_p^H \mathbf{D}_m \mathbf{h}_{sr}|^2$ from the BS to IRS and then to users is given by

$$\bar{f}_X(x) = \frac{2x^{\frac{Q-1}{2}}}{\Gamma(Q) (\sqrt{\Omega_{sr}\Omega_{rm}})^{Q+1}} K_{Q-1} \left(2\sqrt{\frac{x}{\Omega_{sr}\Omega_{rm}}}\right), \quad (\text{A.4})$$

where $\bar{f}_X(x)$ denotes the PDF of unsorted cascade channel gain. Furthermore, we perform integral processing on the above formula and express the corresponding CDF $\bar{F}_X(x)$ as

$$\bar{F}_X(x) = \frac{2}{\Upsilon} \int_0^x y^{\frac{Q-1}{2}} K_{Q-1} \left(2\sqrt{\frac{y}{\Omega_{sr}\Omega_{rm}}}\right) dy, \quad (\text{A.5})$$

where $\Upsilon = \Gamma(Q) (\sqrt{\Omega_{sr}\Omega_{rm}})^{Q+1}$.

Based on (A.5), using $y = xt$ and [35, Eq. (6.561.8)], $\bar{F}_X(x)$ can be calculated as follows:

$$\begin{aligned} \bar{F}_X(x) &= \frac{2}{\Upsilon} \int_0^1 (\sqrt{xt})^{Q-1} K_{Q-1} \left(2\sqrt{\frac{xt}{\Omega_{sr}\Omega_{rm}}}\right) x dt \\ &\stackrel{\sqrt{t} \triangleq y}{=} \frac{4x^{\frac{Q+1}{2}}}{\Upsilon} \int_0^1 y^Q K_{Q-1} \left(2\sqrt{\frac{x}{\Omega_{sr}\Omega_{rm}}} y\right) dy \\ &= 1 - \frac{2}{\Gamma(Q)} \left(\frac{x}{\Omega_{sr}\Omega_{rm}}\right)^{\frac{Q}{2}} K_Q \left(2\sqrt{\frac{x}{\Omega_{sr}\Omega_{rm}}}\right). \quad (\text{A.6}) \end{aligned}$$

Upon substituting (A.6) into (A.3), the CDF $F_X(x)$ of the cascade channel gain can be given by

$$\begin{aligned} F_X(x) &= \phi_m \sum_{l=0}^{M-m} \binom{M-m}{l} \frac{(-1)^l}{m+l} \left[1 - \frac{2}{\Gamma(Q)}\right] \\ &\quad \times \left(\frac{x}{\Omega_{sr}\Omega_{rm}}\right)^{\frac{Q}{2}} K_Q \left(2\sqrt{\frac{x}{\Omega_{sr}\Omega_{rm}}}\right)^{m+l}, \quad (\text{A.7}) \end{aligned}$$

where $\phi_m = \frac{M!}{(M-m)!(m-1)!}$.

Combining (A.7) and (A.2), the probability $\Pr(W_p)$ can be further expressed as follows:

$$\begin{aligned} \Pr(W_p) &= \frac{\phi_m}{\Omega_I} \sum_{l=0}^{M-m} \binom{M-m}{l} \frac{(-1)^l}{m+l} \int_0^\infty \left[1 - \frac{2}{\Gamma(Q)}\right] \\ &\quad \times \left(\frac{\psi_m^* \varphi}{\Omega_{sr}\Omega_{rm}}\right)^{\frac{Q}{2}} K_Q \left(2\sqrt{\frac{\psi_m^* \varphi}{\Omega_{sr}\Omega_{rm}}}\right)^{m+l} e^{-\frac{y}{\Omega_I}} dy, \quad (\text{A.8}) \end{aligned}$$

where $\varphi = (\varpi \rho y + 1)$. Assuming $x = \frac{y}{\Omega_I}$, and using Gauss-Laguerre integration [40, Eq. (25.4.45)], the probability $\Pr(W_p)$ can be given by

$$\begin{aligned} \Pr(W_p) &\approx \phi_m \sum_{l=0}^{M-m} \sum_{u=1}^U \binom{M-m}{l} \frac{(-1)^l H_u}{m+l} \left[1 - \frac{2}{\Gamma(Q)}\right] \\ &\quad \times \left(\frac{\psi_m^* \Lambda}{\Omega_{sr}\Omega_{rm}}\right)^{\frac{Q}{2}} K_Q \left(2\sqrt{\frac{\psi_m^* \Lambda}{\Omega_{sr}\Omega_{rm}}}\right)^{m+l}, \quad (\text{A.9}) \end{aligned}$$

where $\Lambda = (\varpi \rho \Omega_I x_u + 1)$, H_u is the weight of the Gauss-Laguerre integration. r_u is the u -th zero of Laguerre polynomial $L_U(r_u)$ and the corresponding the u -th weight is given by $H_u = \frac{(U!)^2 r_u}{[L_{U+1}(r_u)]^2}$.

Upon substituting (A.9) into (A.1), we can obtain (9). The proof is completed.

APPENDIX B: PROOF OF THEOREM 2

Upon substituting $\varpi = 0$ into (22), the ergodic rate of the m -th user with pSIC for IRS-NOMA networks can be written as

$$\begin{aligned} R_{m,erg}^{pSIC} &= \mathbb{E} \left\{ \log \left(1 + \max_{\mathbf{v}_p} \underbrace{\frac{\rho |\mathbf{v}_p^H \mathbf{D}_m \mathbf{h}_{sr}|^2 a_m}{\rho |\mathbf{v}_p^H \mathbf{D}_m \mathbf{h}_{sr}|^2 \bar{a}_m + 1}}_{\bar{Y}} \right) \right\} \\ &= \frac{1}{\ln 2} \int_0^\infty \frac{1 - F_{\bar{Y}}(y)}{1 + y} dy. \quad (\text{B.1}) \end{aligned}$$

Let $\bar{Y} = \frac{\rho |\mathbf{v}_p^H \mathbf{D}_m \mathbf{h}_{sr}|^2 a_m}{\rho |\mathbf{v}_p^H \mathbf{D}_m \mathbf{h}_{sr}|^2 \bar{a}_m + 1}$ and the CDF $F_{\bar{Y}}(y)$ can be expressed as

$$F_{\bar{Y}}(y) = \Pr \left[|\mathbf{v}_p^H \mathbf{D}_m \mathbf{h}_{sr}|^2 < \frac{y}{\rho(a_m - y\bar{a}_m)} \right], \quad (\text{B.2})$$

where $a_m > y\bar{a}_m$. Upon substituting (A.7) into (B.2) and using Binomial theorem, the CDF $F_{\bar{Y}}(y)$ is given by

$$F_{\bar{Y}}(y) = \phi_m \sum_{l=0}^{M-m} \sum_{r=0}^{m+l} \binom{M-m}{l} \binom{m+l}{r} \frac{(-1)^{l+r}}{m+l} \times \left(\frac{2}{\Gamma(Q)} \right)^r \left[\left(\frac{y\varphi_m}{(a_m - y\bar{a}_m)} \right)^{\frac{Q}{2}} K_Q \left(2\sqrt{\frac{y\varphi_m}{(a_m - y\bar{a}_m)}} \right) \right]^r, \quad (\text{B.3})$$

where $\varphi_m = \frac{1}{\rho\Omega_{sr}\Omega_{rm}}$.

For IRS-NOMA with 1-bit coding scheme, $\mathbf{v}_p^H \mathbf{D}_m \mathbf{h}_{sr}$ and $\mathbf{v}_l^H \mathbf{D}_m \mathbf{h}_{sr}$ are independent and identically distribution for $p \neq l$. As a consequence, the CDF $F_Y(y)$ can be given by

$$F_Y(y) = \left\{ \phi_m \sum_{l=0}^{M-m} \sum_{r=0}^{m+l} \binom{M-m}{l} \binom{m+l}{r} \times \frac{(-1)^{l+r}}{m+l} \left[\frac{2}{\Gamma(Q)} \left(\frac{y\varphi_m}{(a_m - y\bar{a}_m)} \right)^{\frac{Q}{2}} \times K_Q \left(2\sqrt{\frac{y\varphi_m}{(a_m - y\bar{a}_m)}} \right) \right]^r \right\}^P. \quad (\text{B.4})$$

Upon substituting (B.4) into (B.1), the CDF $F_Y(y)$ can be expressed as follows:

$$R_{m,erg}^{pSIC} = \frac{1}{\ln 2} \int_0^{\frac{a_m}{\bar{a}_m}} \frac{1}{1+y} \left\langle 1 - \left[\phi_m \sum_{l=0}^{M-m} \sum_{r=0}^{m+l} \binom{M-m}{l} \binom{m+l}{r} \frac{(-1)^{l+r}}{m+l} \left[\frac{2}{\Gamma(Q)} \left(\frac{y\varphi_m}{(a_m - y\bar{a}_m)} \right)^{\frac{Q}{2}} \times K_Q \left(2\sqrt{\frac{y\varphi_m}{(a_m - y\bar{a}_m)}} \right) \right]^r \right] \right\rangle dy. \quad (\text{B.5})$$

By further applying the Gauss-Chebyshev quadrature [41] on the above equation, we can obtain (24). The proof is completed.

APPENDIX C: PROOF OF THEOREM 3

Upon substituting $\varpi = 0$ into (23), the ergodic rate of the M -th user with pSIC for IRS-NOMA networks can be written as

$$R_{M,erg}^{pSIC} = \mathbb{E} \left[\log \left(1 + \rho a_M \max_{\mathbf{v}_p} \underbrace{(\mathbf{v}_p^H \mathbf{D}_M \mathbf{h}_{sr})^2}_Z \right) \right] = \frac{\rho a_M}{\ln 2} \int_0^\infty \frac{1 - F_Z(z)}{1 + z\rho a_M} dx. \quad (\text{C.1})$$

Denoting $\bar{Z} = |\mathbf{v}_p^H \mathbf{D}_M \mathbf{h}_{sr}|^2$, by the virtue of Order Statistic theory and (A.6), the CDF $F_{\bar{Z}}(z)$ of the M -th user is given by

$$F_{\bar{Z}}(z) = \left[1 - \frac{2}{\Gamma(Q)} \left(\frac{z}{\Omega_{sr}\Omega_{rM}} \right)^{\frac{Q}{2}} K_Q \left(2\sqrt{\frac{z}{\Omega_{sr}\Omega_{rM}}} \right) \right]^M. \quad (\text{C.2})$$

Similar to the procedure in (B.4), we randomly select a column \mathbf{v}_p from \mathbf{V} to maximize \bar{Z} . Hence the CDF $F_Z(z)$ can be given by

$$F_Z(z) = \left[1 - \frac{2}{\Gamma(Q)} \times \left(\frac{z}{\Omega_{sr}\Omega_{rM}} \right)^{\frac{Q}{2}} K_Q \left(2\sqrt{\frac{z}{\Omega_{sr}\Omega_{rM}}} \right) \right]^{MP}. \quad (\text{C.3})$$

Applying the Binomial theorem in (C.3), the CDF $F_X(x)$ can be further rewritten as follow:

$$F_Z(z) = \sum_{r=0}^{MP} \binom{MP}{r} (-1)^{r+1} \left[\frac{2}{\Gamma(Q)} \times \left(\frac{z}{\Omega_{sr}\Omega_{rM}} \right)^{\frac{Q}{2}} K_Q \left(2\sqrt{\frac{z}{\Omega_{sr}\Omega_{rM}}} \right) \right]^r. \quad (\text{C.4})$$

By substituting (C.4) and after some manipulates, we can obtain (25). The proof is completed.

REFERENCES

- [1] Y. Liu, Z. Qin, M. ElKashlan, Z. Ding, A. Nallanathan, and L. Hanzo, "Non-orthogonal multiple access for 5G and beyond," *Proceedings of the IEEE*, vol. 105, no. 12, pp. 2347–2381, Dec. 2017.
- [2] W. Saad, M. Bennis, and M. Chen, "A vision of 6G wireless systems: Applications, trends, technologies, and open research problems," *IEEE Network*, pp. 1–9, Oct. 2019.
- [3] Z. Zhang, Y. Xiao, Z. Ma, M. Xiao, Z. Ding, X. Lei, G. K. Karagiannis, and P. Fan, "6G wireless networks: Vision, requirements, architecture, and key technologies," *IEEE Veh. Technol. Mag.*, vol. 14, no. 3, pp. 28–41, Sep. 2019.
- [4] D. Tse and P. Viswanath, *Fundamentals of wireless communication*, Cambridge University Press, Cambridge, UK, 2005.
- [5] Z. Ding, Y. Liu, J. Choi, Q. Sun, M. ElKashlan, C. L. I, and H. V. Poor, "Application of non-orthogonal multiple access in LTE and 5G networks," *IEEE Commun. Mag.*, vol. 55, no. 2, pp. 185–191, Feb. 2017.
- [6] Z. Ding, Z. Yang, P. Fan, and H. V. Poor, "On the performance of non-orthogonal multiple access in 5G systems with randomly deployed users," *IEEE Signal Process. Lett.*, vol. 21, no. 12, pp. 1501–1505, Dec. 2014.
- [7] X. Yue, Z. Qin, Y. Liu, S. Kang, and Y. Chen, "A unified framework for non-orthogonal multiple access," *IEEE Trans. Commun.*, vol. 66, no. 11, pp. 5346–5359, Nov. 2018.
- [8] Z. Ding, M. Peng, and H. V. Poor, "Cooperative non-orthogonal multiple access in 5G systems," *IEEE Commun. Lett.*, vol. 19, no. 8, pp. 1462–1465, Aug. 2015.
- [9] C. Zhong and Z. Zhang, "Non-orthogonal multiple access with cooperative full-duplex relaying," *IEEE Commun. Lett.*, vol. 20, no. 12, pp. 2478–2481, Dec. 2016.
- [10] X. Yue, Y. Liu, S. Kang, A. Nallanathan, and Z. Ding, "Exploiting full/half-duplex user relaying in NOMA systems," *IEEE Trans. Commun.*, vol. 66, no. 2, pp. 560–575, Feb. 2018.
- [11] Y. Liu, Z. Ding, M. ElKashlan, and H. V. Poor, "Cooperative non-orthogonal multiple access with simultaneous wireless information and power transfer," *IEEE J. Sel. Areas Commun.*, vol. 34, no. 4, pp. 938–953, Apr. 2016.
- [12] X. Liang, Y. Wu, D. W. K. Ng, Y. Zuo, S. Jin, and H. Zhu, "Outage performance for cooperative noma transmission with an af relay," *IEEE Commun. Lett.*, vol. 21, no. 11, pp. 2428–2431, Nov. 2017.
- [13] J. Men, J. Ge, and C. Zhang, "Performance analysis of non-orthogonal multiple access for relaying networks over Nakagami- m fading channels," *IEEE Trans. Veh. Technol.*, vol. 66, no. 2, pp. 1200–1208, Feb. 2017.
- [14] X. Yue, Y. Liu, S. Kang, and A. Nallanathan, "Performance analysis of NOMA with fixed gain relaying over Nakagami- m fading channels," *IEEE Access*, vol. 5, pp. 5445–5454, Mar. 2017.
- [15] Q. Y. Liao, C. Y. Leow, and Z. Ding, "Amplify-and-forward virtual full-duplex relaying-based cooperative noma," *IEEE Wireless Communications Letters*, vol. 7, no. 3, pp. 464–467, Jun. 2018.

- [16] X. Yue, Y. Liu, Y. Yao, X. Li, R. Liu, and A. Nallanathan, "Secure communications in a unified non-orthogonal multiple access framework," *IEEE Trans. Wireless Commun.*, vol. 19, no. 3, pp. 2163–2178, Mar. 2020.
- [17] Y. Liu, Z. Qin, Y. Cai, Y. Gao, G. Y. Li, and A. Nallanathan, "UAV communications based on non-orthogonal multiple access," *IEEE Wireless Commun.*, vol. 26, no. 1, pp. 52–57, Feb. 2019.
- [18] X. Yan, H. Xiao, C. Wang, K. An, A. T. Chronopoulos, and G. Zheng, "Performance analysis of NOMA-based land mobile satellite networks," *IEEE Access*, vol. 6, pp. 31 327–31 339, Jun. 2018.
- [19] J. Zhao, "A survey of intelligent reflecting surfaces (IRSs): Towards 6G wireless communication networks with massive MIMO 2.0," 2019. [Online]. Available: <http://arxiv.org/abs/1907.04789v2>.
- [20] T. Cui, M. Qi, X. Wan, J. Zhao, and Q. Cheng, "Coding metamaterials, digital metamaterials and programmable metamaterials," *Light: Science & Applications*, vol. 3, no. 10, Oct. 2014.
- [21] Q. Wu and R. Zhang, "Towards smart and reconfigurable environment: Intelligent reflecting surface aided wireless network," *IEEE Commun. Mag.*, vol. 58, no. 1, pp. 106–112, Jan. 2020.
- [22] E. Basar, M. Di Renzo, J. de Rosny, M. Debbah, M. Alouini, and R. Zhang, "Wireless communications through reconfigurable intelligent surfaces," *IEEE Access*, vol. 7, pp. 116 753–116 773, Aug. 2019.
- [23] E. Bjornson, O. Ozdogan, and E. G. Larsson, "Intelligent reflecting surface vs. decode-and-forward: How large surfaces are needed to beat relaying?" 2019. [Online]. Available: <https://arxiv.org/abs/1906.03949>.
- [24] M. D. Renzo, K. Ntontin, F. H. D. J. Song, X. Qian, F. Lazarakis, J. de Rosny, D.-T. Phan-Huy, O. Simeone, R. Zhang, M. Debbah, G. Lerosey, M. Fink, S. Tretyakov, and S. Shamai, "Reconfigurable intelligent surfaces vs. relaying: Differences, similarities, and performance comparison," 2020. [Online]. Available: <https://arxiv.org/abs/1908.08747v2>.
- [25] M. Cui, G. Zhang, and R. Zhang, "Secure wireless communication via intelligent reflecting surface," *IEEE Wireless Commun. Lett.*, vol. 8, no. 5, pp. 1410–1414, Oct. 2019.
- [26] C. Huang, A. Zappone, G. C. Alexandropoulos, M. Debbah, and C. Yuen, "Reconfigurable intelligent surfaces for energy efficiency in wireless communication," *IEEE Trans. Wireless Commun.*, vol. 18, no. 8, pp. 4157–4170, Aug. 2019.
- [27] B. Zheng, Q. Wu, and R. Zhang, "Intelligent reflecting surface-assisted multiple access with user pairing: NOMA or OMA?" *IEEE Commun. Lett.*, vol. 24, no. 4, pp. 753–757, Apr.
- [28] M. Fu, Y. Zhou, and Y. Shi, "Intelligent reflecting surface for downlink non-orthogonal multiple access networks," in *IEEE Proc. of Global Commun. Conf. (GLOBECOM)*, Waikoloa, USA, Dec. 2019, pp. 1–6.
- [29] G. Yang, X. Xu, and Y.-C. Liang, "Intelligent reflecting surface assisted non-orthogonal multiple access," 2019. [Online]. Available: <https://arxiv.org/abs/1907.03133>.
- [30] X. Mu, Y. Liu, L. Guo, J. Lin, and N. Al-Dhahir, "Exploiting intelligent reflecting surface in multi-antenna aided NOMA systems," 2019. [Online]. Available: <https://arxiv.org/abs/1910.13636v1>.
- [31] Z. Ding and H. V. Poor, "A simple design of IRS-NOMA transmission," *IEEE Commun. Lett.*, to appear in 2020.
- [32] Z. Ding, R. Schober, and H. V. Poor, "On the impact of phase shifting designs on IRS-NOMA," to appear in 2020.
- [33] T. Hou, Y. Liu, Z. Song, X. Su, Y. Chen, and L. Hanzo, "Reconfigurable intelligent reflecting surface aided NOMA networks," 2019. [Online]. Available: <https://arxiv.org/abs/1912.10044v1>.
- [34] H. A. David and H. N. Nagaraja, *Order Statistics*, 3rd ed. New York: John Wiley, 2003.
- [35] I. S. Gradshteyn and I. M. Ryzhik, *Table of Integrals, Series and Products*, 6th ed. New York, NY, USA: Academic Press, 2000.
- [36] A. A. Nasir, X. Zhou, S. Durrani, and R. A. Kennedy, "Relaying protocols for wireless energy harvesting and information processing," *IEEE Trans. Wireless Commun.*, vol. 12, no. 7, pp. 3622–3636, Jul. 2013.
- [37] J. N. Laneman, D. N. C. Tse, and G. W. Wornell, "Cooperative diversity in wireless networks: Efficient protocols and outage behavior," *IEEE Trans. Inf. Theory*, vol. 50, no. 12, pp. 3062–3080, Dec. 2004.
- [38] T. Kwon, S. Lim, S. Choi, and D. Hong, "Optimal duplex mode for DF relay in terms of the outage probability," *IEEE Trans. Veh. Technol.*, vol. 59, no. 7, pp. 3628–3634, Sep. 2010.
- [39] H. Liu, H. Ding, L. Xiang, J. Yuana, and L. Zheng, "Outage and ber performance analysis of cascade channel in relay networks," in *Proc. the 9th International Conference on Future Networks and Communications*, India, Feb. 2014, pp. 1–8.
- [40] M. Abramowitz and I. Stegun, *Handbook of Mathematical Functions with Formulas, Graphs, and Mathematical Tables*, New York, NY, USA: Dover, 1972.
- [41] E. Hildebrand, *Introduction to numerical analysis*, New York, NY, USA: Dover, 1987.

